Neumann, A.; Lahajnar, N.; Emeis, K.-C.:

Benthic remineralisation rates in shelf and slope sediments of the northern Benguela upwelling margin

In: Continental Shelf Research (2015) Elsevier

DOI: 10.1016/j.csr.2015.12.009

Benthic remineralisation rates in shelf and slope sediments of the northern Benguela upwelling margin

Andreas Neumann[a 1], Niko Lahajnar[a], and Kay-Christian Emeis[a,b]

[a] University of Hamburg, Institute for Geology, Bundesstraße 55, D-20146 Hamburg, Germany (andreas.neumann@awi.de, niko.lahajnar@uni-hamburg.de)
[b] Helmholtz Zentrum Geesthacht Center for Materials and Coastal Research, Max-Planck Str. 1, D-21502 Geesthacht, Germany (kay.emeis@hzg.de)
[1] Alfred Wegener Institute for Polar and Marine Research, Wadden Sea Station Sylt, Hafenstraße 43, D-25992 List/Sylt, Germany

corresponding author: Andreas Neumann, email: andreas.neumann@awi.de,
phone: +49-4152-87-1837

draft: 2015-12-15

Abstract

The Benguela Upwelling System off Namibia is a region of intensive plankton production. Remineralisation of this biomass frequently causes the formation of an oxygen minimum zone. A part of the organic matter is further deposited on the broad shelf in form of an extensive mudbelt with high TOC concentrations. During February 2011 we retrieved sediment samples from shelf and slope sediment along the Namibian coast to establish fluxes of nutrients, oxygen, and N_2 on the basis of pore water concentrations. In mudbelt sediment, fluxes were estimated as high as 8 mmol NH_4^+ m^{-2} d^{-1} and 0.9 mmol PO_4^{3-} m^{-2} d^{-1}, which is probably attributable to the activity of large sulphur bacteria. Especially phosphate is mobilized from sediment overlain by oxygen deficient bottom water when and where bottom water oxygen concentrations fall below 50 µmol l^{-1}. In comparison to nutrient transport by Southern Atlantic Central Water flowing onto the Namibian shelf, benthic nutrient fluxes of the mudbelt contribute less than 5 % to the nutrient budget of the shelf.

Keywords

Benguela, benthic remineralization, oxygen minimum zone, nutrients

1 Introduction

Nitrogen and phosphorus are two essential macronutrients which are the basis of all biological primary production. Masses and ratios of these nutrients in upwelling waters also govern plankton primary production of surface waters of the Benguela Current off the west coast of southern Africa that is the most productive of the large eastern boundary currents in terms of chlorophyll a concentrations and potential primary production (Carr, 2002). Nitrate and phosphate at close to Redfield ratio of 16:1 are either imported from outside the system with upwelling source waters, or are regenerated from mineralisation of organic matter within the system. Loss of reactive nitrogen to denitrification/anammox in suboxic waters over the shelf and upper continental slope (Tyrell and Lucas, 2002; Kuypers et al., 2005) is believed to be the main cause for the observed shift of nitrate:phosphate ratios of upwelled surface waters to values <16. The apparent N-deficit implies an annual N-loss of up to 2.5 Tg N a^{-1} to which denitrification appears to only contribute 0.25 Tg N a^{-1} (Nagel et al., 2013), and anammox possibly up to 1.4 Tg N a^{-1}.

An alternative or additional reason for the observed N-deficit in the northern Benguela Upwelling System is a selective enrichment of upwelling waters with phosphate leaking from organic-rich sediments (Bailey, 1987). Analyses of nutrient-to-carbon ratios (Flohr et al., 2014) indeed suggest a substantial P-source over the shelf, where P-cycling and phosphogenesis are intense (Goldhammer et al., 2010). On the other hand, activity of sulphur bacteria causes phosphate sequestration by phosphorite formation (Goldhammer 2010), which in turn shifts N:P

ratio toward nitrogen. Should that putative sedimentary phosphate source indeed exist, it must be significant, because N:P ratios in intermediate waters arriving at the shelf break are 16:1, whereas N:P ratios of modified upwelling water are 16:1.6 (Flohr et al., 2014).

The relative contributions of processes consuming reactive nitrogen or adding phosphate to the N:P ratios of modified upwelling water are unknown, a clear incentive to study sediment-water exchange rates and to estimate that part of N-loss attributable to sediment denitrification, and that part of P-gain attributable to P-liberation from sediments. The main objective of the present study thus was to establish fluxes of phosphorous and reactive nitrogen across the sediment water interface, and to estimate the contribution of benthic processes to nutrient recycling and observed apparent N-deficit.

The Benguela Current is the dominant surface current along the Namibian coast and represents the eastern limb of the South Atlantic subtropical gyre (Peterson & Stramma 1991). It starts as equatorward current off Cape of Good Hope and follows the South African coast. It receives water masses mainly from the cold South Atlantic Current, but also from the warm Agulhas Current. At around 27 °S, the Benguela Current broadens and most of the current bends westward to become part of the South Equatorial Current. One branch of the surface current continues northwards along the coast until it joins the Angola Current at the Angola-Benguela Frontal Zone (ABFZ) at around 17 °S. There, both currents are deflected westward to form the southern limb of the Angola Gyre (Stramma & England 1999). The general hydrodynamic setting is perturbed by wind-driven coastal upwelling. The eastern limb of the trade wind system blows parallel to the coast and displaces the surface water westward by Ekman transport (Ekman 1905, Mohrholz et al. 2008). A poleward undercurrent of waters high in nutrients and CO_2 and low in oxygen (South Atlantic Central Water, SACW) compensates the general northward surface flow and mixes over the shelf with relatively fresh and oxygenated Eastern South

Atlantic Central Water (ESACW) (Mohrholz et al. 2001) As a consequence, the cross-shelf return flow transports water with reduced oxygen concentration and increased nutrient concentrations across sediments on the shelf and into the upper water column. Unlike other eastern boundary currents, the coastal branch of the Benguela Current flows over a broad continental shelf offshore Namibia. The 100 m isobath is about 50 km offshore at 23 °S, which enables intensive interaction of sediment and bottom water. As the Benguela is highly productive (Silió-Calzada et al. 2008), immense amounts of organic matter accumulate in a mud belt in relatively shallow water in depths between 100 – 200 m (Inthorn et al. 2006).

2 Materials and Methods

2.1 Study site and sampling

The samples were retrieved during the cruise MSM 17/3 of the RV *Maria S. Merian* along the Namibian continental margin in February 2011, which is the season of low upwelling intensity (Shannon 1985) and low primary production rates (Silió-Calzada et al. 2008). The working area (Figure 1) comprises the continental shelf and slope between Lüderitz (26° 40’ S) and the Kunene River mouth (17° 15’ S).

Undisturbed sediment cores were retrieved with a multicorer (Oktopus Kiel) equipped with acrylic tubes (PMMA) with an inner diameter of 10 cm and a length of 60 cm. This sampler recovers bottom-water directly overlying the sediment, permitting to measure concentration profiles of dissolved gases across the water-sediment interface directly after the retrieval of the sediments cores and on board the ship (see below). Pore water was sampled with rhizon core solution samplers (Rhizosphere Research) using core liners prepared with sealed sampling ports

at 1 cm spacing. The rhizon samplers were conditioned in deionized water and connected to sterile, disposable syringes. The first few hundred microliters of the sampled pore water were discarded for flushing and removing any air bubbles. Pore water aliquots for nutrients analysis were transferred to evacuated Exetainers (Labco) and stored at -20°C. Additional cores were sliced in 1 cm intervals and stored at -20°C for CHN analysis and determinations of water content and grain size distribution.

2.2 Sediment characteristics

The frozen sediment slices were freeze-dried in the home laboratory, and the resulting weight loss was used to calculate the water content. The volumetric porosity was calculated from the water content, assuming a mean grain density of 2.65 g cm^{-3}. A subsample of the dry residues was used to determine the concentrations of total nitrogen and organic carbon with an Elemental Analyzer (Carlo Erba NA 1500) calibrated against acetanilide.

2.3 Measurement of dissolved gases

The oxygen concentration profiles were measured within minutes after retrieval of the sediment cores. The supernatant bottom water was adjusted to 10 cm height prior to the profiling, and multiple profiles across the sediment-water interface were measured with an autonomous micromanipulator (Pyro Science) and needle-type microoptodes (Presens, Oxy50) connected to a Microx TX3 (Presens). The sensor was calibrated for each profile individually to account for the constant abrasion of the sensor tip. The sensor readings in the anoxic sediment (0% oxygen saturation) and in air-equilibrated standard (100% oxygen saturation) were used for a two-point calibration.

Concentration profiles of dissolved N_2 and argon (Ar) were measured simultaneously with a quadrupole mass spectrometer (InProcess Instruments, GAM 200) equipped with a needle-type membrane inlet guided by a second micromanipulator (Pyro Science). The needle-type membrane inlet was constructed according to Thomas & Lloyd (1995) and Lloyd et al. (1996). The sensing tip was an orifice (0.2 mm^2) drilled into a stainless steel capillary (0.4 mm outer diameter, 0.2 mm inner diameter). This orifice was covered with a piece of silicone tubing (Silastic, Dow Corning). The stainless steel capillary with the membrane covered orifice was soldered to a 1.5 m long stainless steel transfer capillary (1/16“ outer diameter) of which a section was wound to a coil to serve as an in-line cryo-trap that was cooled with liquid nitrogen. The transfer capillary was connected to the mass spectrometer with a Swagelok connector. Argon was measured as mass to charge ratio m/z 40 and used according to Kana et al. (1994) as reference for N_2 (m/z 28). The concentrations of Ar and N_2 were calibrated with a three-point calibration with air-equilibrated temperature-salinity standards (Kana et al. 1994). Both setups were placed in temperature controlled laboratories to prevent warming-related changes of reaction rates within the sediment cores. The channel m/z 34 was additionally monitored as a qualitative indicator for the presence of H_2S. However, we made no attempt to calibrate for H_2S to get concentration profiles.

2.4 Pore water nutrient analysis

The frozen pore water samples in septum-capped Exetainers (Labco) were thawed in a water bath at room temperature in the home laboratory. Samples were then acidified with 6 M hydrochloric acid (1% v/v final concentration) to stabilize any gaseous ammonia as ammonium. Aliquots were then withdrawn with syringes through the septum and analyzed with a nutrient autoanalyzer (AA3, Seal Analytical) with methods according to Grasshoff et al. (1983).

2.5 Calculations

Reaction rates and diffusive fluxes across the sediment-water interface were calculated on the basis of Fick's 1st law of diffusion (Fick 1855). We employed the algorithm of Berg et al. (1998) to concentration profiles within the sediment, which uses the whole concentration profile for flux calculations. The local effective diffusion coefficients were corrected for porosity and temperature. The actual sediment surface was in most cases between the pre-drilled sampling ports of the core liners and hence the coarse spatial resolution of the pore water samples and porosity measurements fail to record adequately the transition between bottom water and top sediment layer. In our experience, this circumstance tends to introduce artefacts into the flux calculations by the Profile algorithm of Berg et al. (1998) and thus we excluded the bottom water concentrations from flux calculations.

Results of flux calculations were statistically analysed with the software SPSS. For correlation analysis, Spearman's correlation of rank-transformed values was preferred to Pearson's correlation of untransformed values because Spearman's correlation does not presuppose linearity and is less sensitive to outliers (Gideon & Hollister 1987). Isosurface maps were generated with the software Ocean Data View (Schlitzer 2011) using the DIVA method (Troupin et al. 2012).

The apparent nitrogen deficit (N*) was calculated as the difference between observed concentrations of dissolved inorganic nitrogen compounds (DIN) and an hypothetical, initial DIN concentration assumed on the basis of observed phosphate concentrations (P) and an theoretical ratio of N:P = 16 (Deutsch et al. 2001, Tyrell & Lucas 2002).

$$N^* = (16 \times c_{pho}) - c_{DIN}$$

equation 1:

N*: apparent nitrogen deficit

c_{pho}: observed phosphate concentration

c_{DIN}: observed nitrate + ammonium concentration

3 Results

3.1 General description of sediment properties

The surface sediment generally had a high porosity (average: 0.86 ± 0.1) and high TOC concentrations ranging from 0.3% dry weight (station 268) to 9.6% dry weight (station 269). TOC concentrations (range 6 – 10 % dry weight) were highest on the inner shelf between 19°S and 24°S parallel to the coast in a depth interval from 100-250 m. In the area at 26.5 °S (Lüderitz), a local TOC maximum was found in 250-500 m depth (Fig. 3, left). The molar C:N ratio of the surface sediments ranged from 6.9 (station 233) to 11.4 (station 299). The ratio was lowest on the shelf along the coast and highest on the upper continental slope in depths between 250 and 1000 m (Fig. 2, right). Bottom water temperature ranged from 18 °C in shallow coastal water to < 3 °C in deep station along the continental slope. The sediment properties are tabulated in table 1 (master table) and plotted in figure 3. The occurrence of large sulphur bacteria such as *Thiomargarita*, *Beggiatoa*, and *Thioploca* was noted by unaided eye at five shelf stations in oxygen deficient water, but these bacteria were not generally spotted in the sampled mud belt sediment.

3.2 Oxygen at the sediment-water interface

Bottom water oxygen concentrations were indicative of the predominant water type. The bottom water in depths >1,000 m was dominated by North-Atlantic Deep Water (NADW) and had high oxygen concentrations of up to 238 µmol l^{-1}. The shallow stations on the shelf were dominated by South-Atlantic Central Water (SACW) and generally had oxygen concentrations below 60 µmol l^{-1}. The bottom water oxygen was below detection limit at 19°S (Rocky Point), and in the area between 23.5°S (Walvis Bay) and 26.5°S (Lüderitz). An exception to the general pattern of low oxygen concentrations in shallow water was station 268 (23 m), where mixing with well-oxygenated surface water led to a bottom water oxygen concentration of 98 µmol l-1.

Diffusive oxygen uptake correlated significantly with bottom water oxygen concentration (r_s = 0.48, $p < 0.01$, N = 30), so that distribution of oxygen consumption rates had a pattern similar to the distribution of oxygen in the bottom water (Fig. 6). At an ambient concentration of 168 µmol O_2 l^{-1} in bottom water, oxygen uptake was 3.5 ± 1.2 mmol m^{-2} d^{-1} opposed by only 0.3 ± 0.4 mmol m^{-2} d^{-1} at 2 µmol l^{-1} bottom water concentration. Oxygen consumption rates decreased sharply toward 0 mmol m^{-2} d^{-1} where bottom water concentrations were below 40 µmol l^{-1} (Fig. 5). However, this trend was not statistically significant for the whole dataset (r_s=0.29, p=0.12, N=30). Similarly, diffusive oxygen flux and bottom water temperature had no significant correlation (r_s=-0.25, p>0.18).

3.3 Nutrient fluxes across the sediment-water interface

Concentrations of solutes in pore waters were high at shallow water depths on the shelf and upper slope, and decreased with water depth. Phosphate fluxes across the sediment-water

interface estimated from pore-water concentration profiles were always directed into the water column and were lowest at the deepest stations (station 241: -1 µmol PO_4^{3-} m^{-2} d^{-1}). Rates of phosphate release and the resulting phosphate concentration in the bottom water increased with increasing temperature (r_s = -0.45, p 0.005) towards shallower water, peaked at station 229 (820 µmol PO_4^{3-} m^{-2} d^{-1}), and decreased again at temperatures >15°C (see also table 1). Similar to phosphate, ammonium concentrations and fluxes were low at deep stations (station 211: -1 µmol NH_4^+ m^{-2} d^{-1}), but also increased with increasing temperature (r_s = -0.62, $p < 0.001$), peaked at station 224 (8,750 µmol NH_4^+ m^{-2} d^{-1}), and decreased at temperatures >15°C. In contrast to temperature, the TOC concentration of sediments had no correlation with the fluxes of either phosphate (r_s = -0.19, p = 0.26) or ammonium (r_s = -0.19, p = 0.27). The spatial patterns of concentrations and fluxes of phosphate and ammonium are displayed in figures 7 and 8.

The highest nitrate concentrations in the bottom water were observed at stations on the upper slope between 250 m and 500 m water depth, which were influenced by nitrate-rich Antarctic Intermediate Water (AAIW) and cold SACW at temperatures below 10 °C. The average nitrate concentration was 35 µmol l^{-1} and peaked at station 234 at 87 µmol l^{-1}. Diffusive nitrate fluxes into the sediment correlated with bottom water nitrate concentration (r_s = 0.33, p = 0.06), and highest nitrate consumption rates (Fig 5) of up to 700 µmol m^{-2} d^{-1} were observed at stations with highest nitrate concentrations and situated on the upper continental slope (see also table 2). Concentrations and consumption rates of nitrate decreased with decreasing temperature (r_s = -0.56, $p < 0.001$) and increasing bottom depth, and nitrate fluxes ultimately changed direction at the deepest stations (241, 310, 316). There, nitrate was released into the water column at an average rate of -90 µmol NO_3^- m^{-2} d^{-1}. Nitrate consumption rates also increased with decreasing oxygen concentrations (rs = 0.53, p 0.001), but differing from dissolved oxygen, nitrate was never depleted at any of the stations. Nitrite was virtually absent in the bottom water at most stations, although the pore waters of all deep stations had internal nitrite maxima of up to 4 µmol

l^{-1} (at station 272). These sediments released nitrite at rates of up to 10 µmol m^{-2} d^{-1} (Fig 5). Nitrite concentrations in anoxic bottom water of the shelf at 19 °S and 24 °S were increased up to 1 µmol l^{-1}, and the sediment here consumed nitrite from the water column at rates of up to 18.5 µmol m^{-2} d^{-1} at station 225 (Fig 5). The spatial concentration and flux patterns of nitrate and nitrite are displayed in figures 9 and 10. All benthic nutrient fluxes are tabulated in table 1, the statistical analysis is summarized in table 2.

3.4 Nutrient stoichiometry

The apparent nitrogen deficit N* in the bottom water overlying the sediment was calculated as the difference between expected DIN concentration based on phosphate and observed DIN concentrations (equation 1). The calculated N* values varied from 5 µmol N l^{-1} in cold oxygen-rich water and 250 µmol N l^{-1} in warm and oxygen-depleted water (table 1).

3.5 Production of N_2

N_2 production in the sediment calculated from N_2/Ar profiles ranged from 61 µmol (station 295) to 1,274 µmol N_2 m^{-2} d^{-1} (station 271). The mean N_2 fluxes did not correlate significantly with either temperature or with oxygen, nitrate or organic carbon concentrations. Instead, the averaged N_2 fluxes appear to have a complex relation with temperature. The highest N_2 fluxes were observed in the temperature interval 8-14 °C whereas N_2 fluxes decrease at lower as well as higher temperatures (figure 5), mirroring the averaged nitrate uptake rates. N_2 fluxes had a minimum in the dissolved oxygen concentration interval 100-200 µmol O_2 l^{-1}, whereas nitrate fluxes correlated linearly with oxygen concentrations. It is of note that N_2 effluxes are substantially higher than nitrate influxes.

4 Discussion

The broad continental shelf off Namibia accumulates massive amounts of fresh organic matter in the form of an extensive mud belt. There, benthic remineralisation complements pelagic remineralisation and releases nutrients back into the bottom water. This study aimed to establish nutrient fluxes between bottom water and surface sediment of the Benguela Upwelling System to estimate the contribution of benthic remineralisation to overall nutrient supply. The results further enable to estimate the contribution of benthic processes to the nutrient budget and the observed apparent nitrogen deficit in upwelled water, which subsequently hosts primary production.

4.1 Intensity of benthic remineralisation

We examined the control of remineralisation of organic matter in sediments by amount and quality of organic matter as electron acceptors, availability of electron donors such as oxygen and nitrate, and the temperature.

We observed a TOC distribution with an extended mud belt on the inner shelf between 19 °S and 24 °S and a deeper depocenter at 27 °S agrees with the general TOC distributions reported by Mollenhauer et al. (2002) and Inthorn et al. (2006). Degradation of this organic matter releases the major nutrient elements phosphorus and nitrogen primarily as phosphate and ammonium, but their observed fluxes were at first glance unrelated to organic carbon concentrations in this study. Remineralisation rates driven by bacteria and invertebrates are positively correlated with water temperature (e.g., Kristensen et al. 1992), which in turn varies with water depth. As expected, the

temperature had a significant impact on the diffusive fluxes of phosphate (Spearman r_s: -0.45, p = 0.005) and ammonium (r_s: -0.62, $p < 0.001$) in our data set, and the fluxes of both compounds increased exponentially with temperature (Fig. 5 and Tab. 1).

It has to be noted that temperature had a very close correlation with water depth (Fig. 2) and it is thereby difficult to discriminate effects of temperature and depth. As for a depth-related effect, particulate organic matter deposited in greater water depths was transported for a longer period than particles in shallow water, and degradation has therefore proceeded further. This relation of depth and reactivity is reflected in the higher C:N ratio of sediment in 400…1000 m. Less degraded organic matter in shallow sediment with C:N ratio close to the initial Redfield ratio of 6.6 can sustain higher fluxes of ammonium and phosphate than more degraded organic matter in similarly low oxygen concentrations (Fig. 5). However, the C:N ratio of the bulk organic matter is a rather coarse proxy of reactivity, but a more sensitive proxy such as amino acid-based Reactivity Index (RI) or Degradation Index (DI) is not yet available for the sampled sediment.

The highest fluxes of ammonium and phosphate were observed in sediment of the inner mud belt at bottom depths < 400 m and temperatures < 14 °C, whereas coastal sediment in water temperatures > 15 °C had significantly lower efflux of ammonium and phosphate. These coastal stations had an average TOC content of 2.0 ± 1.4 %, and thus significantly less organic matter than sediment of the inner mud belt (TOC= 6.1 ± 3.2 %). Although an overall analysis of TOC concentration with phosphate ($r_s = 0.19$, p = 0.26) and ammonium flux ($r_s = 0.19$, p = 0.27) is not statistically significant, remineralisation is still governed by substrate quality. This is reflected in the correlation of ammonium efflux with the sediment C_{org}:N_{tot} ratio (r_s = -0.55, $p < 0.001$), implying that fresh organic matter with low C:N ratio releases more ammonium than refractory organic matter with high C:N ratio (Tab. 2).

The phosphate efflux from continental slope sediment is similar to results of Zabel et al. (1998), which examined deep sea sediment in the southern Atlantic. Ammonium and phosphate fluxes are further in a similar magnitude as the results of Berelson et al. (1987) and Jahnke (1990) from upper slope sediment off California (Tab. 3). Our results from shelf sediment are in good agreement with preceding studies from Joubert (2006), Bohlen et al. (2011), Noffke et al. (2012), and Dale et al. (2014) covering different oxygen minimum zones (Tab. 3).

The ratio of produced ammonium and phosphate (6.0 ± 6.7) is below the average N : P ratio of primary producers (N : P ≈ 16, Redfield et al. 1963), which constitute the bulk of sedimentary organic matter. Although organic-bound nitrogen and phosphorous are not necessarily remineralized and released in equal ratios, the deviation is worth closer examination. The highest phosphate fluxes were observed at stations along the inner mud belt (Fig. 5, 7) and agree with results of previous studies (Schulz & Schulz 2005, Goldhammer et al. 2010, Goldhammer et al. 2011). These authors attribute the intensive phosphate release to activity of abundant *Thiomargarita* sulphur bacteria. These bacteria store phosphate while oxygen is available and scavenge phosphate from the water column to restock internal phosphate upon resuspension (Schulz & Jørgensen 2001). Phosphate released by *Thiomargarita* thus is not necessarily remineralized where it is released. Episodic oxygen depletion triggers pulses of phosphate mobilisation from intracellular depots of these bacteria and instantaneously increases pore-water phosphate concentrations, so that phosphate minerals such as carbonate apatite precipitate (Goldhammer et al. 2010). This precipitated phosphate accumulates in the mud belt, which ultimately turns the sediment into a phosphate sink. A significant part of dissolved phosphate, however, diffuses into the bottom water, together with ammonium that is not consumed in the sediment. The ratio of released ammonium and phosphate depends not only on the ratio of phosphate release and sequestration but also on the extent of nitrification in the presence of oxygen, which may be detected by internal concentration maxima of nitrate and nitrite (not

shown). This recycled nitrate effluxes deep sediment at temperatures < 3 °C (Fig. 5), while at the same time fuelling denitrification that produces N_2. Thus, N_2 production scales more with bottom water oxygen concentration than with nitrate concentration. N_2 production makes the sediment a sink for reactive nitrogen, although reactive nitrogen received as nitrate or particulate organic matter is not completely converted to N_2. Recycled nitrogen is released into the water column as nitrate at high oxygen concentration, while ammonium is released at low oxygen concentration.

The N_2 production rates track the elimination of reactive nitrogen via denitrification or anammox. In our data set, N_2 production generally exceeded nitrate consumption by an average factor of 7.4 ($n=19$, $\sigma=9.7$). This excess N_2 production cannot simply be accounted to anammox that has a theoretical ratio of N_2 production to NOx consumption of 2. Instead, the excess N_2 production illustrates the effect of coupled nitrification-denitrification within the sediment. Nitrification is effective in deep and cold sediments to compensate nitrate consumption and to cause net release of nitrate from the sediment into the water column at the expense of ammonium release. Tyrell and Lucas (2002) observed the largest nitrate deficit in the water column at 12-13°C water temperature, in line with maximum rates of nitrate consumption and N_2 production at 11-14 °C in our study (Fig. 5).

4.2 The effect of large sulphur bacteria

The shelf sediment of the Benguela Upwelling System is well-known for the occurrence of large sulphur bacteria such as *Thiomargarita* and *Beggiatoa*. These bacteria store nitrate, sulphur, and phosphate in large internal vacuoles (Schulz & Jørgensen 2001) and can affect the benthic cycling of N and P considerably. If these bacteria are exposed to hydrogen sulphide, they reduce the stored nitrate to ammonium via DNRA (dissimilatory nitrate reduction to ammonium), and use internal polyphosphate depots to gain energy without an electron acceptor (Schulz et al.

2005). As a result, *Thiomargarita* and *Beggiatoa* can release significant amounts of ammonium and phosphate into the sediment pore water (Schulz & Schulz 2005, Goldhammer et al. 2010, 2011). We visually observed *Thiomargarita* filaments and *Beggiatoa* mats on the sediment of 6 of 50 sampled stations. However, we certainly missed less obvious populations, especially if they were buried in the sediment as in the case of *Thiomargarita* (Schulz & Schulz 2005). Therefore we inspected the porewater profiles for subsurface peaks of ammonium and phosphate which should indicate the presence of said sulphur bacteria. We found such subsurface phosphate peaks in all bottom depths along the entire coast as mapped in figure 11 c. In shelf sediment, the phosphate peaks were accompanied by ammonium peaks and may indeed indicate the presence of sulphur bacteria (Fig. 11 a), and the high effluxes of ammonium and phosphate from shelf sediment may therefore be assigned to these sulphur bacteria (Fig. 5 a, b). However, in greater bottom depth of the continental slope we found phosphate peaks without an ammonium peak (Fig. 11 b). But whether these phosphate peaks in slope sediment are result of mobilisation from dissolving iron hydroxide or the activity of microbes cannot be concluded with our data.

Large sulphur bacteria are often reported to consume nitrate and hydrogen sulphide by means of dissimilatory nitrate reduction to ammonium (Fossing et al. 1995, Schulz & Jørgensen 2001). In this mode, reactive nitrogen consumed as nitrate is released back into the water column as ammonium, where efficient nitrification (Füssel et al. 2011) closes a circle in which reactive nitrogen carries oxygen into the sediment. However, our observation of N_2 production in all sampled sediment (Tab. 1, Fig. 4) seems to interfere with this view. This could be a seasonal effect as we sampled the sediment in austral summer, which is a period of weak upwelling and low plankton production. Reduced productivity and reduced flux of fresh organic matter to the sediment might also reduce the rate of benthic sulphate reduction. Since DNRA also consumes H_2S which we noticed only occasionally (Tab. 1), the observed N_2 production might indicate that

DNRA is not the sole pathway of nitrate consumption in periods of weak upwelling. Alternatively, sulphur bacteria might switch from DNRA to denitrification in periods of low H_2S availability, as results of Sweerts et al. (1990) imply.

4.3 Bottom water nutrient stoichiometry

Concentrations of phosphate and dissolved inorganic nitrogen (DIN) in bottom water sampled 1 cm above the sediment surface reflect the net effects of solute fluxes across the sediment water interface. Phosphate accumulation in bottom water samples having oxygen concentrations >40 µmol l^{-1} is locked to oxygen depletion (Fig. 5), which implies that these sediments release the majority of phosphate back into the water column. An apparent phosphate excess was observed where bottom water with 12–15°C and < 40 µmol O_2 l^{-1} hugs the mud belt (Fig 5 and 11). In sediment at these locations we observed substantially increased phosphate release, and similarly high phosphate fluxes into the water column (figure 5 b) have been ascribed to the activity of *Thiomargarita* sulphur bacteria as discussed above (Schulz & Schulz 2005, Goldhammer et al. 2010, Goldhammer et al. 2011). Although it is plausible assuming that these large sulphur bacteria fuel the intensive phosphate release, we cannot verify this assumption on the basis of our observations as we visually detected these bacteria only occasionally (Tab 1) and found no consistent pattern of intense phosphate efflux and the occurrence of large sulphur bacteria.

In contrast to phosphate, fluxes of ammonium are constantly low in sediment with > 400 m bottom depth, which we interpret as sign of nitrification that suppresses the efflux of ammonium. This is supported by subsurface peaks in nitrate concentration (Fig. 4) and efflux of nitrate into the water column (Fig 5). However, ammonium efflux is substantially increased in OMZ-influenced sediment of the shelf, which again might be explained with DNRA activity of sulphur bacteria. On the other hand, the good correlation of ammonium efflux and sediment C:N ratio

(Tab. 2) suggests that the increased ammonium efflux is result of intense degradation of fresh organic matter.

Taken together, a calculated N-deficit (N*) is basically the expression of an imbalance of DIN and phosphate, which might be result of elimination of reactive nitrogen (rN) to N_2, phosphate mobilisation from benthic depots, or both. Our N_2 measurements in the sediment generally show N_2 production and thus the elimination of rN to N_2. As a result, most bottom water N:P ratios fall below the theoretical 16:1 Redfield ratio (Fig 11). Additionally, the calculated N* exceeds 100 µmol N* l^{-1} in some OMZ-influenced locations (Tab. 1), which also exceeds the initial DIN concentration of either NADW or SACW. This suggests additional phosphate mobilisation from benthic depots such as *Thiomargarita* and iron oxy-hydroxides (Goldhammer et al. 2010). It further supports the hypothesis of pronounced phosphate mobilisation from sediment when the bottom water becomes anoxic as recently reported by Flohr et al. (2014). Similarly, our results suggest that pronounced phosphate mobilisation starts when oxygen concentration falls below 40 µmol O_2 l-1. Bottom water anoxia then triggers discharge of labile P stocks and shifts N:P ratio towards phosphorus. Goldhammer et al. (2010, 2011) have shown such pulse-like mobilization of phosphate from sediments exposed to anoxia. However, the efflux of phosphorus mobilized from oxygen-sensitive stocks eventually ceases when these stocks are depleted, even though bottom water anoxia may still prevail. This may be the reason why some of our samples as well as the samples presented in Flohr et al. (2014) had no apparent excess phosphate despite low oxygen concentrations. The direct consequence of this presumed pulsed P-release from the mud belt is that episodic sampling (as is typical for ship-based research) is likely to miss such P pulses, which effectively aliases the true N-loss when estimated on the basis of N:P ratios.

4.4 Significance of benthic fluxes for the nutrient budget of the Benguela Upwelling System

Two recent publications (Nagel et al., 2013; Flohr et al., 2014) quantified the nitrate deficit generated in the OMZ over the shelf and upper slope. Nagel et al. (2013) extrapolated the N-deficit to 2.5 Tg a^{-1} (6.9 x 10^9 mol N d^{-1}) from N:P ratios, but found that only 10% of this was due to denitrification tracked by changes in the isotopic ratios of nitrate. The estimate of N-loss is similar to that established by Kuypers et al. (2005), who estimated that anammox accounts for elimination of 1.4 ± 1 Tg N a^{-1} (3.8 x 10^9 mol N d^{-1}). Likewise, Flohr et al. (2014) postulate on the basis of dissolved inorganic carbon to nutrient ratios that the sediment contribution to dissolved P in upwelling water is roughly 60%.

However, both results exceed the benthic fluxes of the present study by several orders of magnitude and underline the dominance of water column processes over benthic fluxes. Fluxes of DIN and phosphate from mud belt sediment into the bottom water are high in comparison to fluxes in the remaining study area and are used here for a rough extrapolation. Assuming that the mud belt comprises 15.000 km^2 and that the median effluxes of 630 µmol NH_4^+ m^{-2} d^{-1} and 80 µmol PO_4^{3-} m^{-2} d^{-1} (< 400 m, < 40 µmol O_2 l^{-1}) are representative, the averaged fluxes of N and P from the sediment to the water column sum up to 1.2 x 10^6 mol P d^{-1} and 9.5 x 10^6 mol N d^{-1}, respectively. These figures are low in comparison to N and P transported into the study area by the coastal Benguela Current. Muller et al. (2014) estimated that 0.54 Sv of SACW and ESACW are transported onto the shelf of the northern Benguela Upwelling System during the austral summer (DJF). Together with typical phosphate and nitrate concentrations of 1.2 µmol PO_4^{3-} l^{-1} and 12.6 µmol NO_3^- l^{-1} (Poole & Tomczak 1999), we calculated a typical transport of 5.6 x 10^7 mol P d^{-1} and 5.9 x 10^8 mol N d^{-1} onto the shelf. Thus, benthic remineralization is probably of minor importance for the nutrient availability in the surface water and even the intense nutrient release from mud belt sediment in conjunction with upwelling of bottom water may influence nutrient availability only temporally and regionally. In support, N:P ratios of bottom water

sampled just above the sediment surface fall close to 12 (Fig. 12), which corresponds to the average N:P ratios of SACW (10.5) and ESCW (9.0) (Poole & Tomczak 1999).

4.5 Limitations and uncertainties

Using concentration profiles to estimate fluxes begs the question whether or not diffusion is the dominant transport mechanism. Alternative transport processes, most prominently advection, potentially exceed diffusive transport by orders of magnitude (e.g. Precht & Huettel 2003). The sediment of the present study generally had high porosities of 0.86 ± 0.1 and consisted of diatom ooze on the continental shelf, gradually being displaced by calcareous ooze as bottom depth increased. These cohesive sediments limit advective movement of pore-water, and argue for diffusion as the dominant transport mechanism. Fossing et al. (2000), on the other hand, argued that bioirrigation of surface sediment on the SW African continental slope contributed significantly to depth-integrated areal sulphate reduction rates. In the same vein, Glud et al. (1994) observed that in-situ oxygen profiles underestimated the total oxygen uptake measured in benthic chambers. However, transport within the impervious, muddy sediment is still constrained in the presence of macrozoobenthos organisms such as worms, and solute exchange is enhanced basically by increasing the specific surface of the sediment (Aller 1980). Since we neglected the effect of macrozoobethos on solute fluxes, our approach thus yields minimum estimates of fluxes at the sediment-water interface. Lastly, undirected diffusion-like transport affects all solutes simultaneously and does not affect the flux ratios.

The profile method for flux estimation is further prone to insufficient spatial resolution. Especially the nitrate penetration depth in highly reactive mudbelt sediment tended being low, and was less than the 1 cm sampling resolution in 5 profiles. An example of this undersampling

is presented in figure 4, station 254. The consequence is that the PROFILE algorithm (Berg et al. 1998) probably underestimated the true fluxes in these cases.

Stations with apparently similar conditions with respect to e.g. temperature, oxygen concentration or TOC content had a marked scatter in calculated fluxes, which is especially true for mud belt stations. This scatter of observed fluxes can at least partly be attributed to spatial heterogeneity of macrozoobenthos diversity and abundance (Mertzen et al., in prep) as well as spatially heterogene occurrence of large sulphur bacteria. This heterogeneity becomes effective as nutrient, oxygen and N_2 were sampled from different cores. Another source of uncertainty is the difference in time scales of the different fluxes. As a substrate, oxygen is rapidly consumed and the inevitable delay between sampling and measurement in the ship's lab might alter concentration profiles considerably. On the other hand, profiles of quasi-stable products such as phosphate, ammonium and N_2 are virtually stable over days or even longer as long as the solute transport is dominated by slow diffusion and production balances the efflux. That includes the possibility that ammonium and phosphate mobilized by a transient anoxia event might not be exported completely into the water column. Instead, the increased ammonium and phosphate concentrations might still prevail in the pore water while the bottom water above the sediment is oxic again. Thus, the different processes in the sediment we sampled with a single snap shot are not necessarily in phase.

5 Conclusions

We estimated the benthic fluxes of nutrients, oxygen, and N_2 on the basis of pore water profiles. The release of ammonium and phosphate increases from low levels at the continental slope to a magnitude of 10^0 mmol NH_4^+ m^{-2} d^{-1} and 10^{-1} mmol PO_4^{3-} m^{-2} d^{-1}. Fluxes of ammonium,

phosphate, nitrate, and N2 are most intense where shelf sediment is influenced by oxygen deficient bottom water, which is probably attributable to the activity of large sulphur bacteria. Factors such as TOC quality and oxygen concentration additionally modulate the nutrient fluxes: Oxygen-depletion triggers pronounced phosphate mobilization of mud belt sediment, low TOC concentrations constrain remineralisation intensity in coastal sediment.

Phosphate mobilization from sediment overlain by sporadically anoxic bottom water is a plausible assumption to explain the time-variable apparent nitrogen deficit (N*) of modified upwelling water that is calculated on the basis of phosphate concentrations (Deutsch et al. 2001, Tyrell & Lucas 2002, Nagel et al. 2013). The results of the present study indicate that phosphate is mobilized when and where bottom water oxygen concentrations fall below 50 µmol l^{-1}.

Acknowledgements

We wish to thank captain and crew of the RV *Maria S. Merian* for excellent support. This study as a part of the GENUS project (BMBF 03F0497A) received financial support by the German Federal Ministry of Education and Research (BMBF). The BMBF had no involvement in conduct of research or preparation of this article. We acknowledge the helpful comments of three anonymous reviewers.

5 References

Aller, R. C. (1980): Quantifying solute distributions in the bioturbated zone of marine sediments by defining an average microenvironment. Geochimica et Cosmochimica Acta, Vol. 44, 1955 – 1965.

Bailey, G.W., 1987. The role of regeneration from the sediments in the supply of nutrients to the euphotic zone in the Southern Benguela System. South African Journal of Marine Science, 5: 273-285.

Berelson, W. M., D. E. Hammond and K. S. Johnson (1987). Benthic fluxes and the cycling of biogenic silica and carbon in two southern borderland California basins. Geochemical Cosmochim. Acta 51: 1345-1363.

Berg P, N. Risgaard-Petersen, and S. Rysgaard (1998). Interpretation of measured concentration profiles in sediment pore water. Limnol. Oceanogr. 43 (7), 1500-1510.

Bohlen, L., A. W. Dale, S. Sommer, T. Mosch, C. Hensen, A. Noffke, F. Scholz, and K. Wallmann (2011): Benthic nitrogen cycling traversing the Peruvian oxygen minimum zone. Geochimica et Cosmochimica Acta 75, 6094-6111.

Carr M.-E. (2002): Estimation of potential productivity in eastern boundary currents using remote sensing. Deep-Sea Res. II 49**,** 59–80,

Dale, A. W., S. Sommer, E. Ryabenko, A. Noffke, L. Bohlen, K. Wallmann, K. Stolpovsky, J. Greinert, and O. Pfannkuche (2014): Benthic nitrogen fluxes and fractionation of nitrate in the Mauritanian oxygen minimum zone (Eastern Tropical North Atlantic). Geochimica et Cosmochimica Acta 134, 234-256.

Deutsch C., N. Gruber, R. M. Key, J. L. Sarmiento, and A. Ganachaud A. (2001): Denitrification and N_2 fixation in the Pacific Ocean. Glob. Biogeochem. Cycles 15, 483–506.

Ekman V.W. (1905): On the influence of the earth's rotation on ocean currents. Arch. Math. Astron. Phys. 2, no. 11.

Flohr A., A. K. van der Plas, K.-C. Emeis, V. Mohrholz, and T. Rixen (2014): Spatio-temporal patterns of C:N:P ratios in the northern Benguela upwelling system. Biogeosciences 11, 885–897.

Fossing H., V. A. Gallardo, B.B. Jørgensen, M Hüttel, L. P. Nielsen, H. Schulz, D. E. Canfield, S. Forster, R. N. Glud, J. K. Gundersen, J. Küver, N. B. Ramsing, A. Teske, B. Thamdrup, and O. Ulloa (1995): Concentration and transport of nitrate by the mat-forming sulfur bacterium Thioploca. Nature 374, 713–715.

Füssel J., P. Lam, G. Lavik, M. M. Jensen, M. Holtappels, M. Günter, and M. M. M. Kuypers (2011): Nitrite oxidation in the Namibian oxygen minimum zone. The ISME Journal, in press.

Gideon R. A. and R. A. Hollister (1987): A rank correlation coefficient resistant to outliers. Journal of the American Statistical Association 82, no. 398, 656-666.

Glud R. N., J. K. Gundersen, B. B. Jorgensen, N. P. Revsbech, and H. D. Schulz (1994): Diffusive and total oxygen uptake of deep-sea sediments in the eastern South Atlantic Ocean: *in situ* and laboratory measurements. Deep-Sea Research 1, vol. 41, no. 11, 1767-1788.

Goldhammer T. V. Brüchert, T. G. Ferdelman, and M. Zabel (2010): Microbial sequestration of phosphorus in anoxic upwelling sediments. Nature Geoscience 3, 557-561.

Goldhammer T., B. Brunner, S. M. Bernasconi, T. G. Ferdelman, and Matthias Zabel (2011): Phosphate oxygen isotopes: Insights into sedimentary phosphorus cycling from the Benguela upwelling system. Geochimica et Cosmochimica Acta 75, 3741–3756.

Grasshoff K., M. Erhardt, and K. Kremling (1983): Methods of Seawater Analysis, Verlag Chemie, Weinheim.

Inthorn, M. T. Wagner, G. Scheeder, and M. Zabel (2006): Lateral transport controls distribution, quality, and burial of organic matter along continental slopes in high-productivity areas. Geology 34, no. 3, 205-208.

Inthorn M., V. Mohrholz, and M. Zabel (2006b): Nepheloid layer distribution in the Benguela upwelling area offshore Namibia. Deep-Sea Research I, vol. 53, 1423–1438.

Jahnke, R. A. (1990): Early diagenesis and recycling of biogenic debris at the seafloor, Santa Monica Basin, California. Journal of Marine Research 48, 413-436.

Joubert W.R. (2006): Seasonal variability of sediment oxygen demand and biogeochemistry on the Namibian inner shelf. M.Sc. Thesis, University of Cape Town, Dept. of Geological Sciences, 97 pp.

Kana T. M., C. Darkangelo, M. D. Hunt, J. B. Oldham, G. E. Bennett, and J. C. Cornwell (1994): Membrane inlet mass spectrometer for rapid high-precision determination of N2, O2, and Ar in environmental water samples. Analytical Chemistry 66, 4166−4170.

Kristensen E., F. Ø. Andersen, and T. H. Blackburn (1992): Effects of benthic macrofauna and temperature on degradation of macroalgal detritus: The fate of organic carbon. Limnology & Oceanography 37, no. 7, 1404-1419.

Kuypers M.M.M., G. Lavik., D. Woebken, M. Schmid, B.M. Fuchs, R. Amann, et al. (2005) Massive nitrogen loss from the Benguela upwelling system through anaerobic ammonium oxidation. Proceedings of the National Academy of Sciences of the United States of America 102: 6478-6483.

Lloyd D., K. Thomas, D. Price, B. O'Neil, K. Oliver,and T. N. Williams (1996): A membrane-inlet mass spectrometer miniprobe for the direct simultaneous measurement of multiple gas

species with spatial resolution of 1 mm. Journal of Microbiological Methods Journal of Microbiological Methods 25, 145-151.

Mohrholz V., M. Schmidt, and J. R. E. Lutjeharms (2001): The hydrography and dynamics of the Angola-Benguela Frontal Zone and environment in April 1999. South African Journal of Marine Science 97, 199–208.

Mohrholz V., C. H. Bartholomae, A. K. van der Plas, and H. U. Lass (2008): The seasonal variability of the northern Benguela undercurrent and its relation to the oxygen budget on the shelf. Continental Shelf Research 28, 424–441.

Mollenhauer G., R. R. Schneider, P. J. Müller, V. Spieß, and G. Wefer (2002): Glacial / interglacial variablity in the Benguela upwelling system: Spatial distribution and budgets of organic carbon accumulation. Global Biogeochemical Cycles 16, no 4, 1134-1149.

Muller A.A., C.J.C. Reason, M. Schmidt, V. Mohrholz , and A. Eggert (2014): Computing transport budgets along the shelf and across the shelf edge in the northern Benguela during summer (DJF) and winter (JJA). Journal of Marine Systems 140, 82–91.

Nagel B., Emeis K.-C., Flohr A., Rixen T., Schlarbaum T., Mohrholz V., and v. d. Plas A.(2014): N-cycling and balancing of the N-deficit generated in the oxygen minimum zone over the Namibian shelf – an isotope-based approach, Journal of Geophysical Research: Biogeosciences, 118, 361–371, doi:10.1002/jgrg.20040.

Noffke, A., C. Hensen, S. Sommer, F. Scholz, L. Bohlen, T. Mosch, M. Graco, and K. Wallmann (2012): Benthic iron and phosphorus fluxes across the Peruvian oxygen minimum zone. Limnology and Oceanography 57, 851-867.

Peterson R. G. and L. Stramma (1991): Upper-level circulation in the South Atlantic Ocean. Progress in Oceanography 26, 1-73.

Poole R. and M. Tomczak (1999): Optimum multiparameter analysis of the water mass structure in the Atlantic Ocean thermocline. Deep-Sea Research I, no. 46, 1895–1921.

Precht E. and M. Huettel (2003): Advective pore-water exchange driven by surface gravity waves and its ecological implications. Limnol. Oceanogr. 48(4), 1674-1684.

Redfield, A. C., B. H. Ketchum, and F. A. Richards (1963): The influence of organisms on the composition of sea water, in The Sea, vol. 2, edited by M. N. Hill, Interscience New York, 26-77.

Reimers, C. E., R. A. Jahnke, and D. C. McCorkle (1992): Carbon fluxes and burial rates over the continental slope and rise off central California with implications for the global carbon cycle. Global Biogeochemical Cycles 6, 199-224.

Schlitzer R. (2011): Ocean Data View. http://odv.awi.de

Schulz, H. N., B. B. Jørgensen (2001): Big Bacteria. Annual Review of Microbiology 55: 105-137.

Schulz H. N. and H. D. Schulz (2005): Large sulfur bacteria and the formation of phosphorite. Science 307, 416-418.

Shannon L.V. (1985): The Benguela ecosystem part 1. Evolution of the Benguela, physical features and processes. Oceanography and Marine Biology: An Annual Review 23, 105–182.

Silió-Calzada A., A. Bricaud, J. Uitz, and B. Gentili (2008): Estimation of new primary production in the Benguela upwelling area, using ENVISAT satellite data and a model dependent on the phytoplankton community size structure. Journal of Geophysical Research, vol. 113, C11023, 1-19.

Stramma L. and M. England (1999): On the water masses and mean circulation of the South Atlantic Ocean. Journal of Geophysical Research 104, no. C9, 20863-20883.

Sweerts, J. P. R. A., D. De Beer, L. P. Nielsen, H. Verdouw, J. C. Van den Heuvel, Y. Cohen, and T. E. Cappenberg (1990): Denitrification by Sulfur Oxidizing Beggiatoa Spp Mats on Fresh-Water Sediments. Nature, 344(6268), 762-763. DOI:10.1038/344762a0

Thomas K. L. and D. Lloyd (1995): Measurement of denitrification in estuarine sediment using membrane inlet mass spectrometry. FEMS Microbiol. Ecol. 16, 103– 114.

Troupin, C., A. Barth, D. Sirjacobs, M. Ouberdous, J.-M., Brankart, P. Brasseur, M. Rixen, A. Alvera Azcarate, M. Belounis, A. Capet, F. Lenartz, M.-E. Toussaint, and J.-M. Beckers (2012): Generation of analysis and consistent error fields using the Data Interpolating Variational Analysis (Diva). Ocean Modelling, 52-53, 90-101.

Tyrell T. and M. I. Lucas (2002): Geochemical evidence of denitrification in the Benguela upwelling system. Continental Shelf Research 22, 2497–2511.

Veraat A. J., J. J. M. de Klein, and M. Scheffer (2011): Warming can boost denitrification disproportionately due to altered oxygen dynamics. PLoS ONE 6, no. 3, e18508.

Zabel M., A. Dahmke, and H. D. Schulz (1998): Regional distribution of diffusive phosphate and silicate fluxes through the sediment-water interface: the eastern South Atlantic. Deep-Sea Research 1, vol. 45, 277-300.

Figure captions

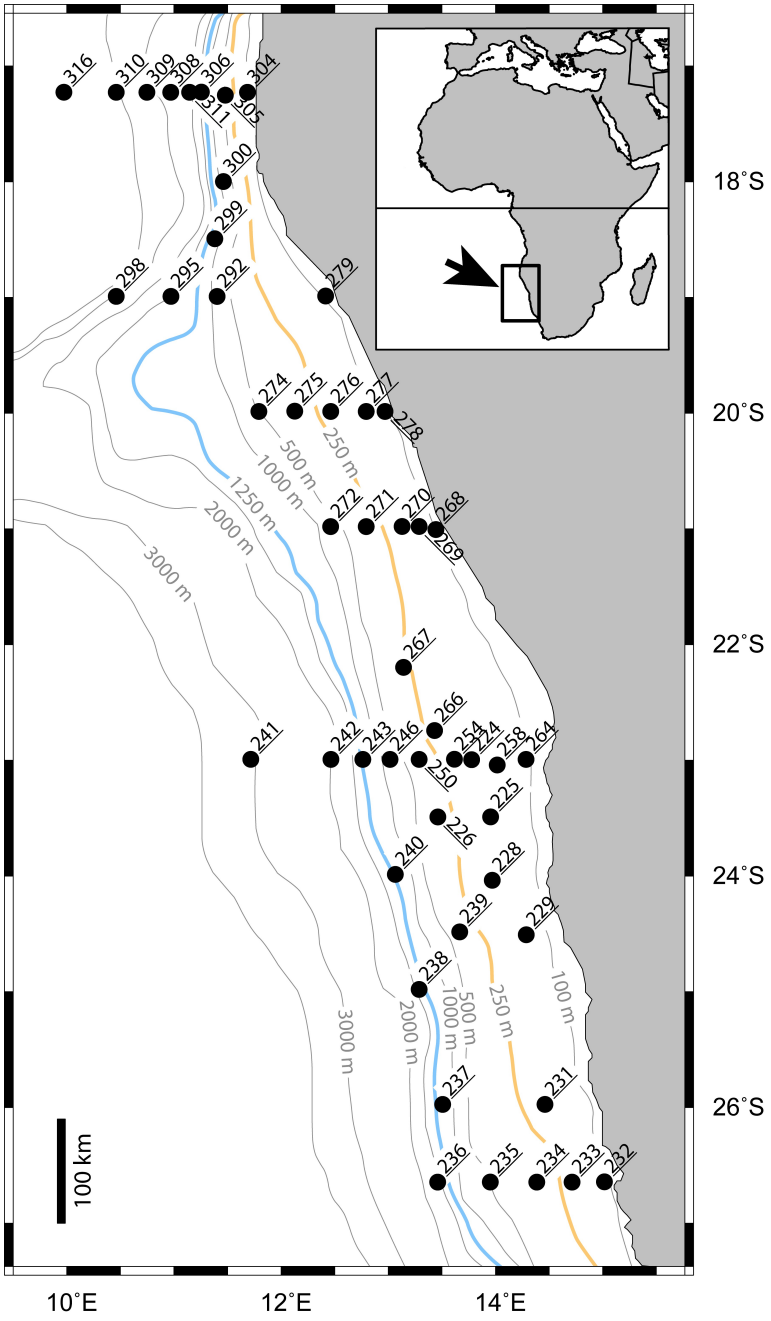

Fig 1: Sampled stations during the cruise MSM 17/3 of the RV Maria S. Merian along the continental shelf and slope off the Namibian coast. The line with orange hue indicates transition between shelf and upper slope at the 250 m isobath, the line with blue hue indicates transition between upper slope and lower slope at 1250 m, respectively. The insert shows the working area (arrow) at the coast of southern Africa.

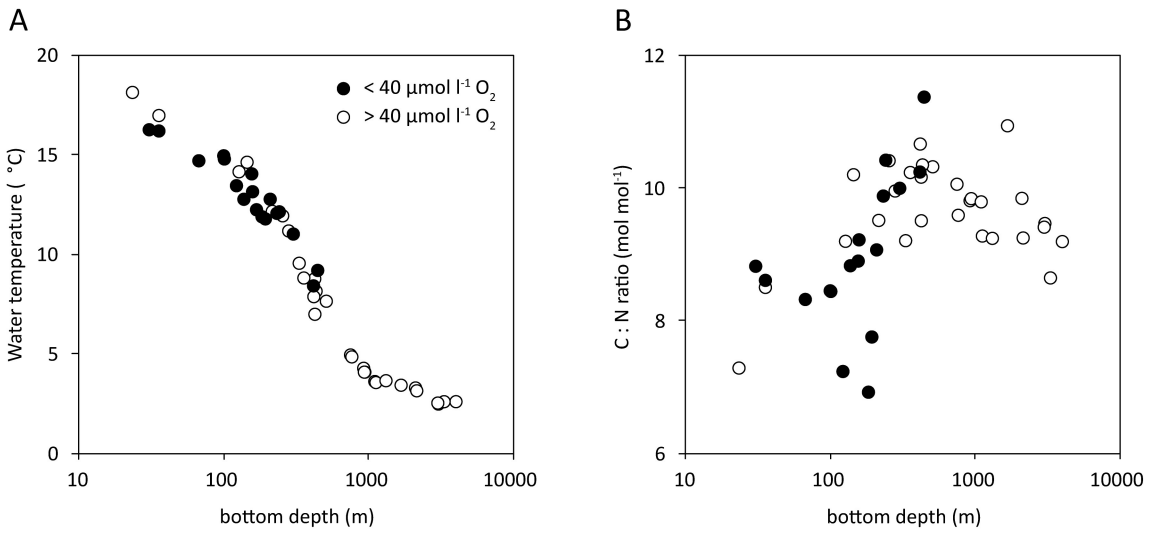

Fig 2: Characteristics of sampled sites. A) Temperature in the bottom water correlates with bottom depth. B) Variation of sediment N_{tot} : C_{org} ratio with bottom depth. Open circles indicate stations with > 40 µmol O_2 l^{-1} in the bottom water, filled circles indicate stations with < 40 µmol O_2 l^{-1} in the bottom water.

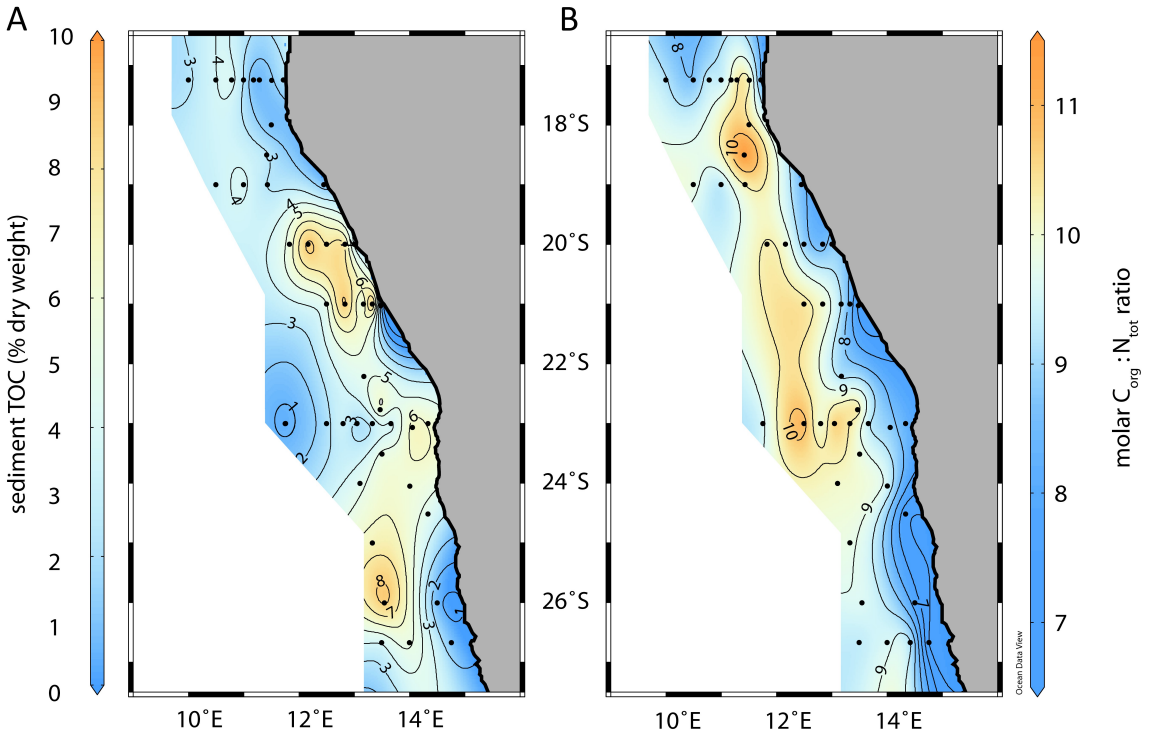

Fig 3: Concentration of TOC in the surface sediment (A), and molar ratio of C_{org} : N_{tot} (B).

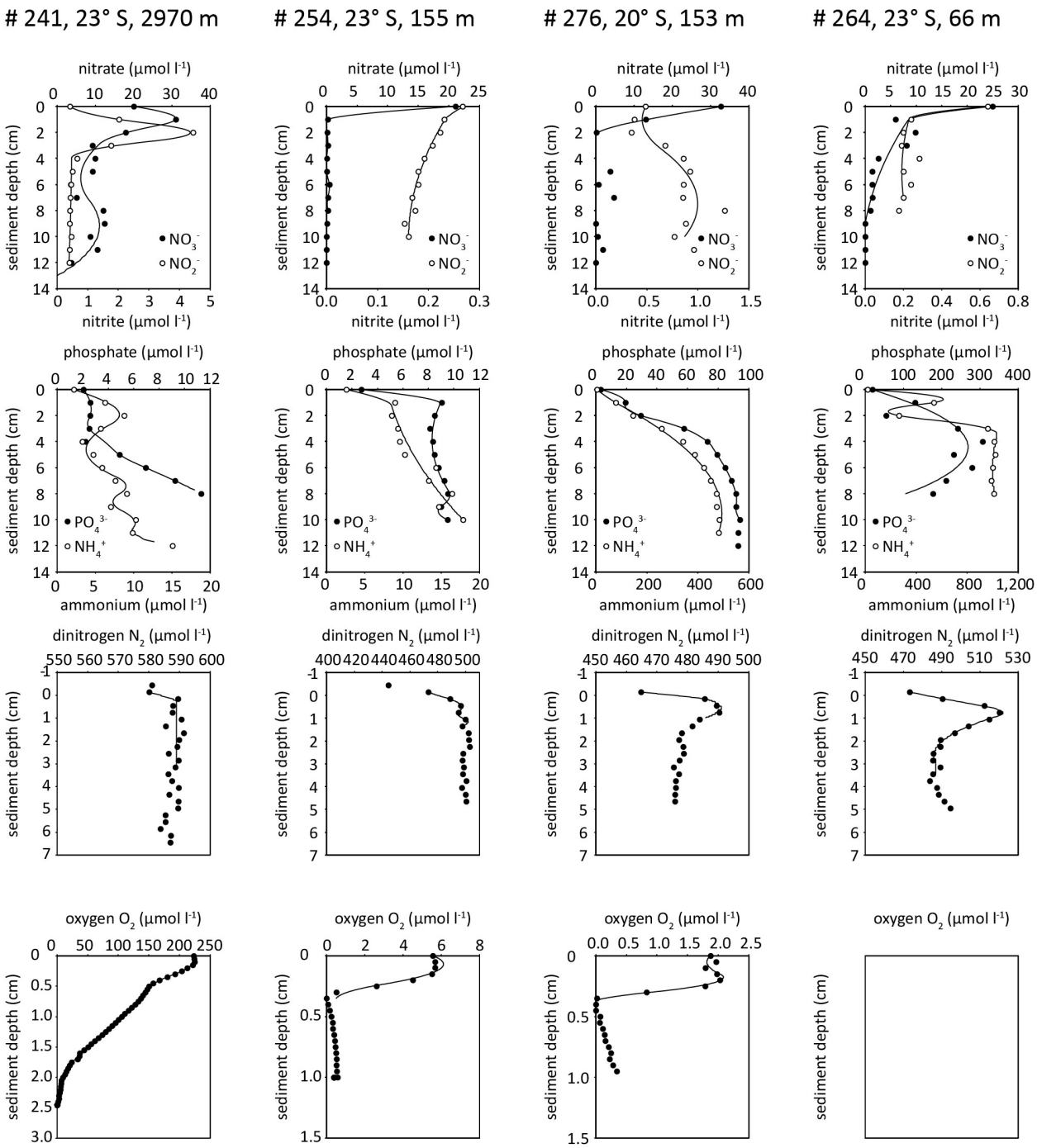

Fig 4: Concentration of nutrients, N_2, and oxygen in sediment of four locations. Open and filled circles indicate actually measured concentrations; the solid lines represent concentration profiles modeled with PROFILE and subsequently used for flux calculations.

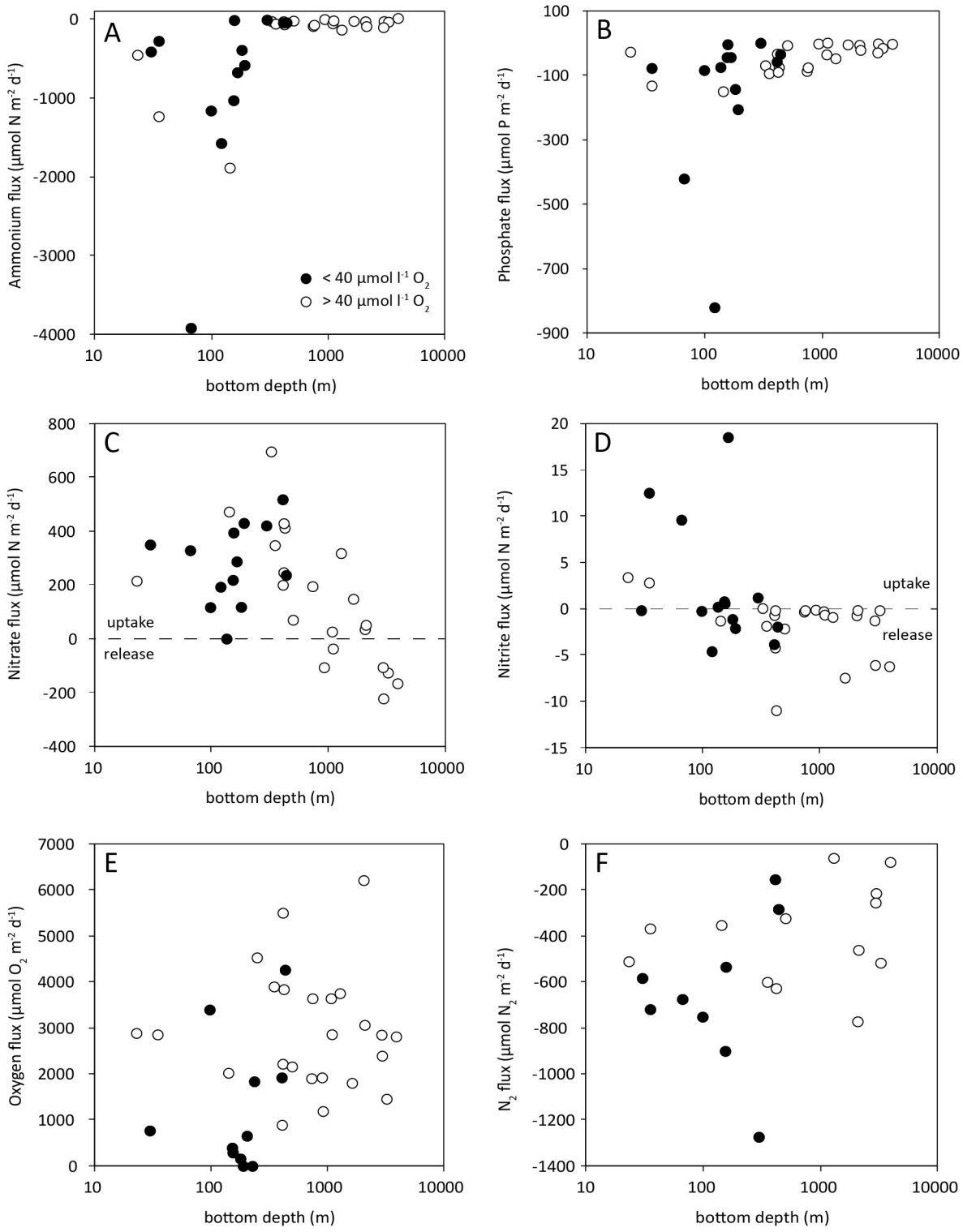

Fig 5: Benthic fluxes of ammonium (A), phosphate (B), nitrate (C), nitrite (D), oxygen (E), and N_2 (F). Open circles indicate stations with > 40 µmol O_2 l^{-1} in the bottom water, filled circles indicate stations with < 40 µmol O_2 l^{-1} in the bottom water.

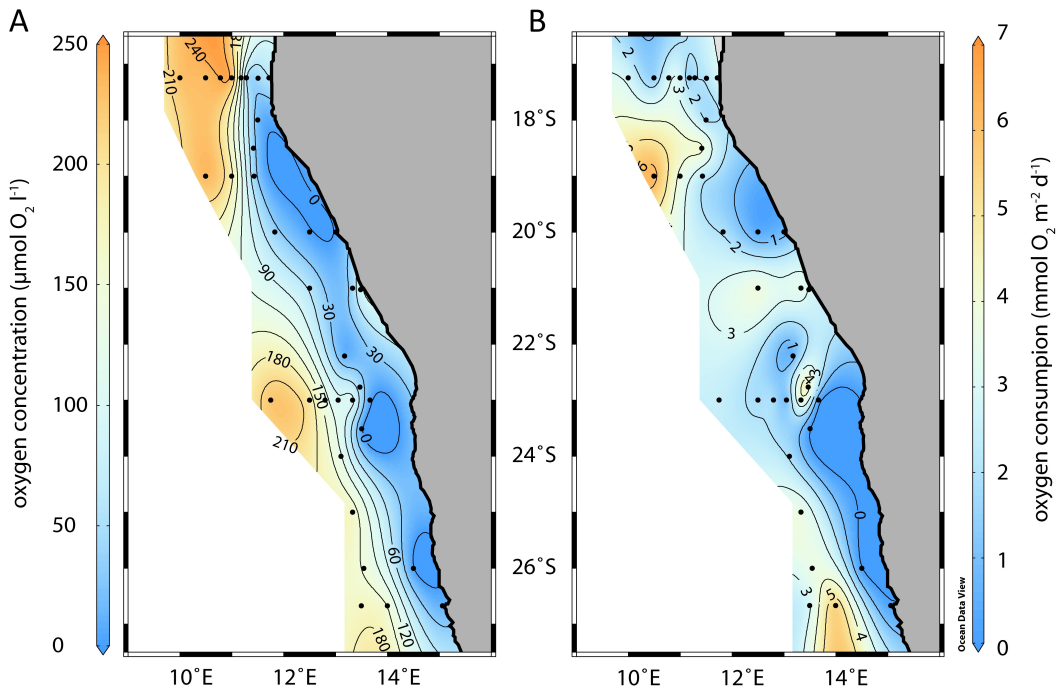

Fig 6: Concentration of dissolved oxygen in the bottom water (A), and benthic oxygen consumption rate (B).

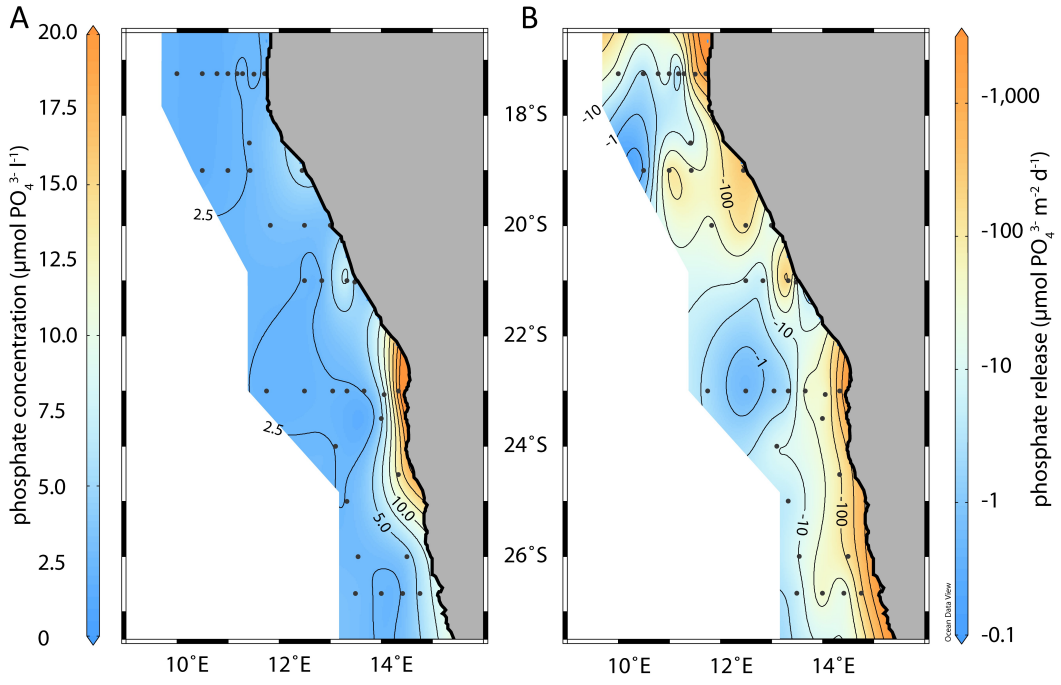

Fig 7: Concentration of phosphate in the bottom water (A), and phosphate flux across the sediment-water interface (B). Negative fluxes denote phosphate export into the water column.

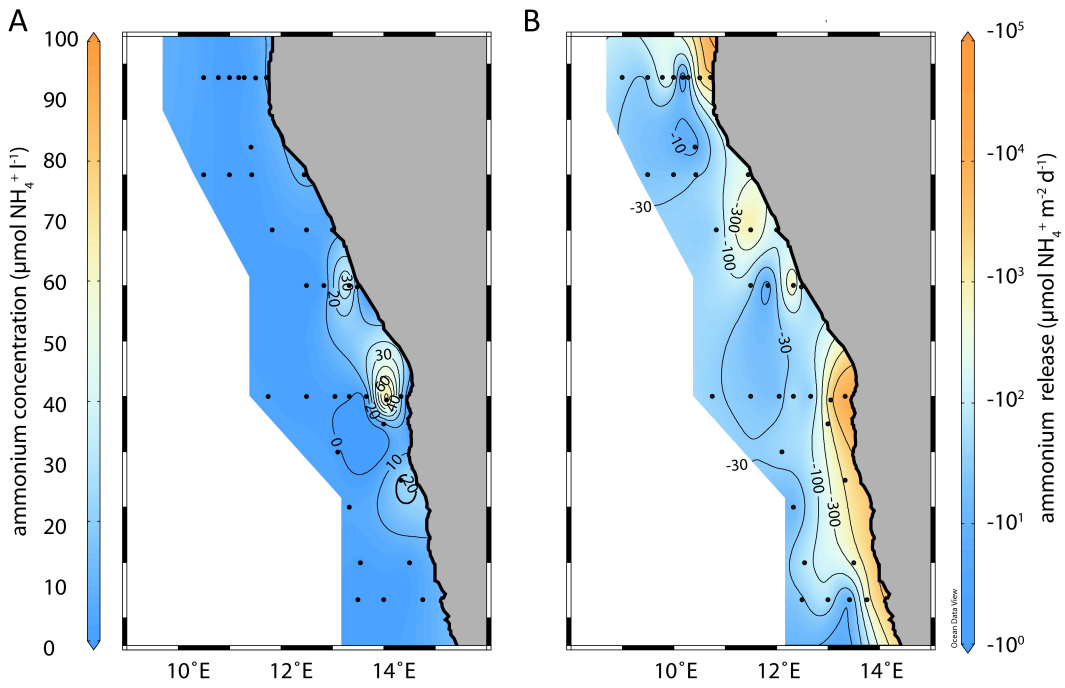

Fig 8: Concentration of ammonium in the bottom water (A), and ammonium flux across the sediment-water interface (B).

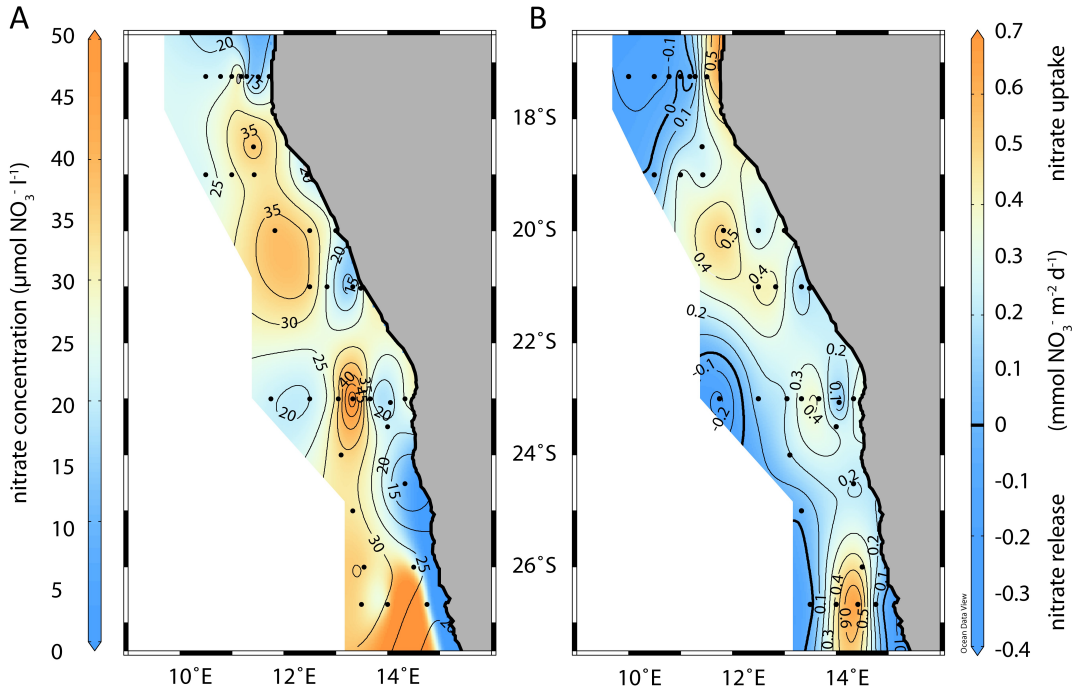

Fig 9: Concentration of nitrate in the bottom water (A), and nitrate flux across the sediment-water interface (B). Positive fluxes denote nitrate consumption, negative fluxes denote nitrate export into the water column.

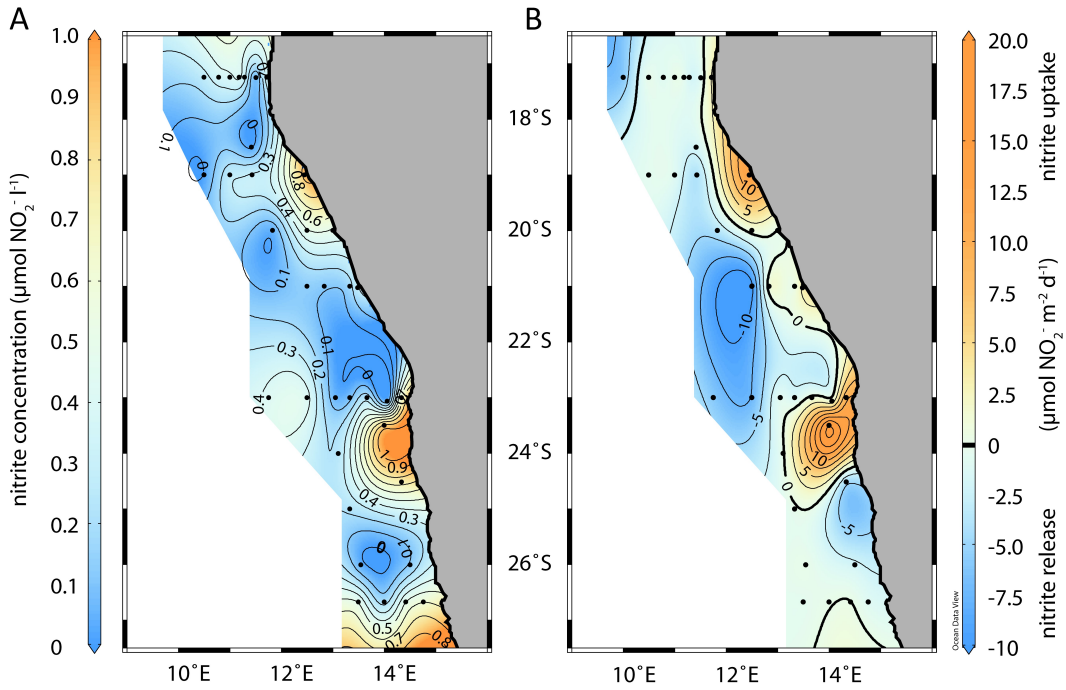

Fig 10: Concentration of nitrite in the bottom water (A), and nitrite flux across the sediment-water interface (B). Negative fluxes denote nitrite export into the water column.

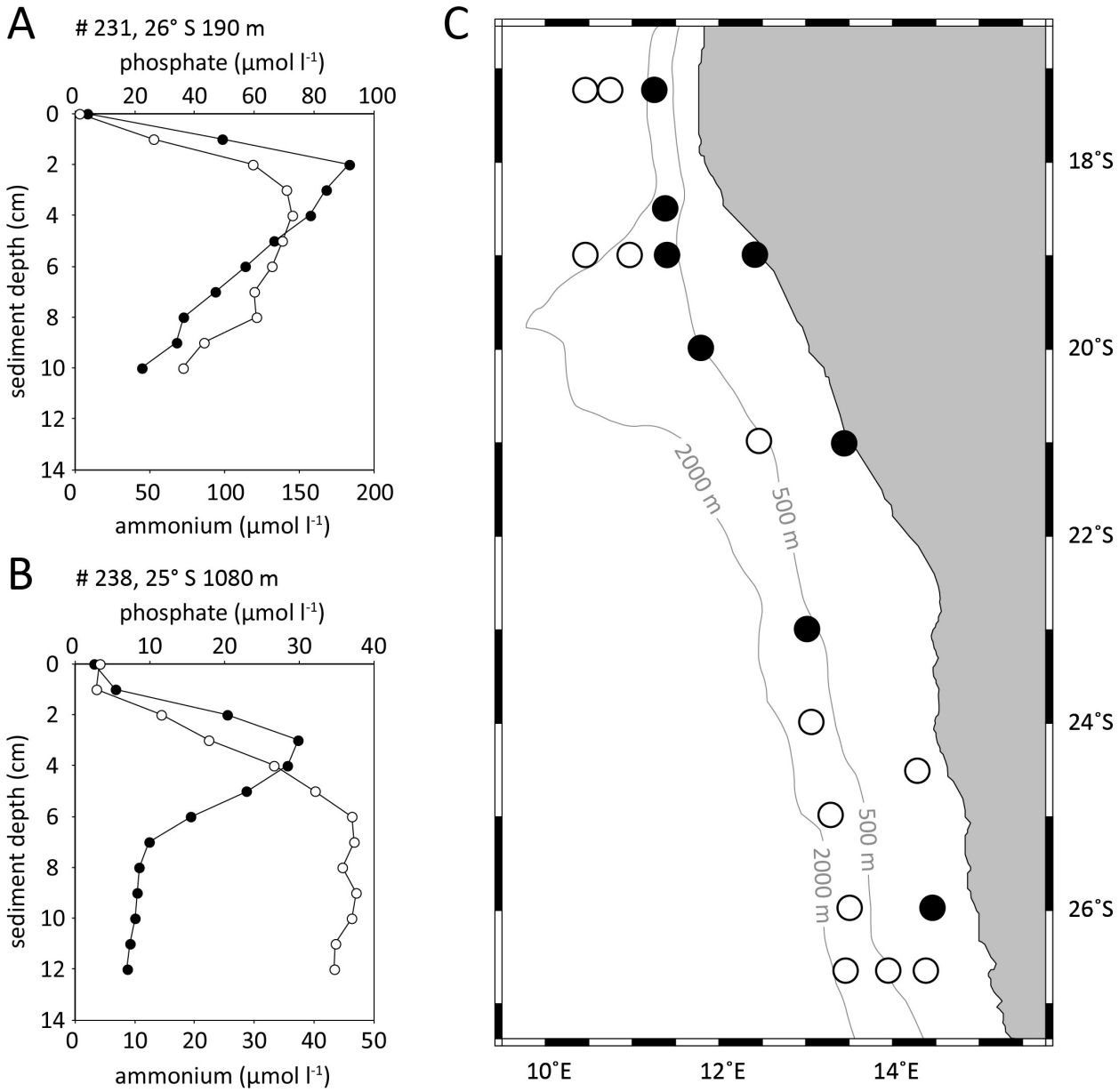

Fig 11: Distribution of subsurface concentration peaks of ammonium and phosphate. A: Case 1 with similar peaks of phosphate (full) and ammonium (open). B: Case 2 phosphate peak (full) without ammonium peak (open). C: Distribution of case 1 (full) and case 2 (open) in sediment off Namibia.

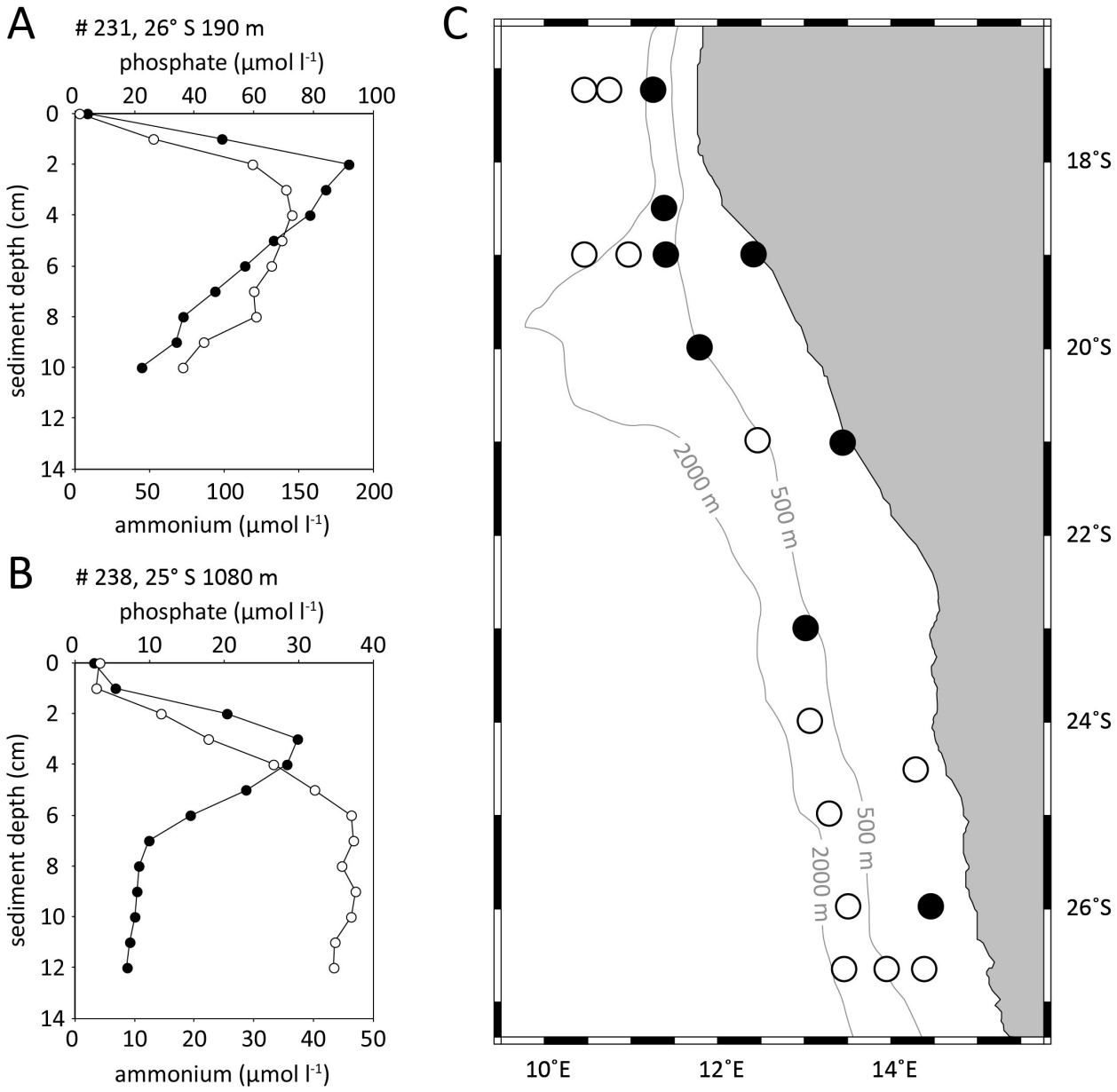

Fig 12: Bottom water stoichiometry of dissolved inorganic nitrogen (DIN) and phosphate. Open circles indicate stations with > 40 µmol O_2 l^{-1} in the bottom water, filled circles indicate stations with < 40 µmol O_2 l^{-1} in the bottom water. The solid line indicates the Redfield ratio of N : P = 16:1, the dashed line indicates a N:P ratio of 12.

Table 1: Characteristics and calculated fluxes in sediment sampled during cruise MSM 17/3 in February 2011. Stations ordered by depth. Negative fluxes are directed from the sediment into the water column, positive fluxes vice versa. Abbreviations for qualitative H_2S observation in upper 5 cm: y = H_2S observed, n = no H_2S observed. Abbreviations for visual inspection of sediment cores for occurrence of large sulfur bacteria: Tm = Thiomargarita, B/T = Beggiatoa / Thioploca mat, n = no large bacteria observed. Missing values are left blank.

station	depth (m)	latitude (deg)	longitude (deg)	temperature (°C)	Bottom water O_2 (µmol l^{-1})	oxygen flux (µmol m^{-2} d^{-1})	N_2 flux (µmol m^{-2} d^{-1})	ammonium flux (µmol m^{-2} d^{-1})	phosphate flux (µmol m^{-2} d^{-1})	nitrate flux (µmol m^{-2} d^{-1})	nitrite flux (µmol m^{-2} d^{-1})	H_2S detected in upper 5 cm	N deficit N* (µmol l^{-1})	sulfur bacteria
268	23	-21.028	13.487	18.2	86	2889	-511	-453	-27	216	3	y	36.2	B / T
278	30	-20.000	13.000	16.3	1	769	-583	-412		350	0	n	22.3	n
279	35	-19.000	12.450	16.2	16		-719	-277	-77		13	n	63.8	n
304	35	-17.250	11.717	17.0	60	2858	-368	-1233	-132		3	y	12.9	n
264	66	-23.000	14.333	14.7	11		-675	-3918	-421	329	10	y	258.2	n
269	98	-21.000	13.333	15.0	39	3398	-751	-1161	-84	117	0	n	75.6	n
277	99	-20.000	12.833	14.8	2									B / T
229	120	-24.512	14.335	13.5	1			-1574	-820	193	-5		181.0	Tm
224	135	-23.063	14.058	12.8	1			-8752	-74	1	0		14.1	n
305	142	-17.253	11.507	14.7	47	2023	-353	-1885	-150	473	-1	n	18.0	n
276	153	-20.000	12.500	14.1	2	396	-900	-1031	-44	219	1	y	12.8	B / T
254	155	-23.000	13.667	13.2	5	290	-534	-13	-4	395	1	n	19.8	n
225	165	-23.500	14.000	12.3	1			-675	-43	288	19		43.3	B / T
233	180	-26.667	14.760	11.9	11	160		-392	-143	119	-1		64.1	n
231	190	-26.000	14.500	11.8	1	0		-583	-205	430	-2		35.8	n
267	205	-22.208	13.180	12.8	10	655								n
226	228	-23.512	13.505	12.1	2	0								n
300	237	-18.000	11.500	12.2	18	1838								n

266	250	-22.765	13.468	12.0	45	4531								n
275	275	-20.000	12.167	11.2										Tm
271	296	-21.000	12.833	11.1	7		-1274	-8	1	421	1	n	9.9	n
234	325	-26.667	14.417	9.6	45			-27	-69	696	0		-46.6	n
250	350	-23.000	13.333	8.9	102	3900	-600	-59	-94	348	-2	n	-20.0	n
274	408	-20.000	11.833	8.5	38	1923	-154	-44	-57	518	-4	n	7.4	n
246	410	-23.000	13.050	7.9	93	893		-28	-33	201	-1		3.4	n
292	416	-19.000	11.433	8.8	41	2219	-627	-43	-33	247	-4	n	8.1	n
235	417	-26.667	14.000	7.0	150	5502		-68	-90	429	0		6.2	n
272	425	-21.000	12.500	8.2	57	3840		-49	-75	412	-11		3.2	n
299	436	-18.500	11.417	9.2	40	4264	-283	-42	-34	237	-2	n	2.8	n
306	500	-17.250	11.288	7.7	43	2161	-323	-20	-7	71	-2	n	30.1	n
240	735	-24.000	13.108	5.0	123	1905		-89	-87	195	0		4.6	n
237	750	-26.000	13.550	4.9	146	3642		-73	-75		0		6.1	n
243	905	-23.000	12.800	4.3	134	1923								n
311	922	-17.250	11.183	4.1	141	1192		-1	-1	-106	0		4.8	n
238	1080	-25.000	13.333	3.7	164	3643		-54	-35	27	0		4.4	n
236	1100	-26.667	13.500	3.6	168	2861		-18	1	-36	-1		12.4	n
295	1290	-19.000	11.000	3.7	187	3753	-61	-134	-47	318	-1	n	5.7	n
242	1640	-23.000	12.500	3.5	194	1805		-25	-4	148	-7		12.6	n
298	2063	-19.000	10.500	3.3	232	6211	-772	-28	-5	36	-1	n	2.9	n
308	2103	-17.250	11.000	3.2	239	3065	-461	-90	-21	52	0	n	5.1	n
309	2939	-17.250	10.783	2.6	238	2852	-255	-103	-29	-105	-1	n	5.5	n
241	2970	-23.000	11.750	2.5	224	2395	-214	-27	-1	-222	-6	n	10.4	n
310	3247	-17.250	10.500	2.6	231	1458	-517	-34	-15	-126	0	n	2.8	n
316	3921	-17.250	10.000	2.6	227	2813	-79	13	-2	-165	-6	n	-17.2	n

Table 2: Spearman correlation coefficients (r_s). Significant results are indicated with * ($p < 0.01$) and ** ($p < 0.001$).

	temperature	TOC	C:N ratio	$[O_2]$	$[NO_3^-]$
PO_4^{3-} flux					
r_s	-0.451 **	0.193	0.279	0.353 *	0.025
p	0.005	0.261	0.099	0.032	0.884
N	36	36	36	36	36
NH_4^+ flux					
r_s	-0.615 **	-0.191	0.551 **	0.430 **	0.342 *
p	< 0.001	0.265	< 0.001	0.008	0.041
N	36	36	36	36	36
NO_3^- flux					
r_s	0.560 **	0.175	0.140	-0.526 **	0.328
p	< 0.001	0.330	0.439	0.001	0.062
N	36	36	36	36	36

Table 3: Comparison of benthic solute fluxes of various oxygen minimum zones. Negative values indicate flux into the sediment. * diffusive flux from pore water gradient, § May-September 2003, & November / December 2002.

Region	Water depth (m)	bottom water O_2 (mM)	TOC (wt %)	Estimated benthic fluxes (mmol m^{-2} d^{-1})				Reference
				O_2	PO_4^{3-}	NO_3^-	NH_4^+	
California Borderland Basins	900 to 1800	6 to 28	3 to 6	-0.5 to -2.6	0.011 to 0.017	-0.8 to 0.03	0.53 to 2	Berelson et al., 1987
Santa Monica Basin	400 to 910	<10	5.4	-0.36±0.18	0.097±0.046	-1.1±0.31		Jahnke, 1990
Peru at 11° S	80 to 1000	0 to 40	3.5 to 15	0 to -2		-3.8 to -0.3	0 to 4	Bohlen et al., 2011
Peru at 11° S	80 to 1000	0 to 40	3.5 to 15		0 to 0.62 *			Noffke et al., 2012
Mauritania at 18° N	50 to 1100	40 to 125	1 to 3	-1.9 to -12.4		-2.24 to +0.66	0 to 1.17	Dale et al., 2014
Benguela 17° to 26.5°S	20 to 3000	2 to 168	0.3 to 9.6	-0.3 to -3.5	0 to 0.82 *	-0.7 to 0.09	0 to 8.75	this study
Benguela at 23°S/14°E	122 to 129	2 to 22	9 to 14	< -20.1 §	0.03 to 0.27 *	-0.61 to 0.04	0.68 to 5.3 &	Joubert, 2006